Macromolecules

Article

pubs.acs.org/Macromolecules

Side Chain Engineering of Polythiophene Derivatives with a Thienylene−Vinylene Conjugated Side Chain for Application in Polymer Solar Cells

Zhi−Guo Zhang, Siyuan Zhang, Jie Min, Chaohua Cui, Hua Geng, Zhigang Shuai, and Yongfang Li*

Beijing National Laboratory for Molecular Sciences, CAS Key Laboratory of Organic Solids, Institute of Chemistry, Chinese Academy of Sciences, Beijing 100190, China

Supporting Information

ABSTRACT: Two new conjugated side-chain isolated polythiophene derivatives, **PT4TV** and **PT4TV-C**, were designed and synthesized by copolymerization of thiophene unit with thienylene−vinylene (TV) conjugated side chain and unsubstituted terthiophene unit. The difference of the two polymers is an additional carbonyl group on the conjugated TV side chain in **PT4TV-C**. Compared to previous reported conjugated side chain polythiophenes (CSC-PTs) with concentrated side chains, **PT4TV** and **PT4TV−C** showed red-shifted and enhanced $\pi-\pi^*$ transition absorption of the polymer backbone along with the shoulder peak and steep absorption edge, indicating ordered polymer main chains and well-packed side chains. **PT4TV** possessed an absorption edge of 663 nm and a HOMO energy level at −5.21 eV. The introducing of electron deficient carbonyl group in **PT4TV−C** led to 17 nm red-shifted absorption and a down-shifted HOMO energy level at −5.26 eV, but aroused the issue of poorer planarity of the polymer backbone. The more ordered structure in **PT4TV** translated into better hole mobility and better photovoltaic properties. The polymer solar cell based on **PT4TV** as donor and indene−C_{60} bisadduct as acceptor displayed a power conversion efficiency of 3.05% with a high open circuit voltage of 0.93 V, under the illumination of AM1.5G, 100 mW/cm^2. The results indicate that the side chain isolated CSC-PTs could be promising high performance photovoltaic polymers.

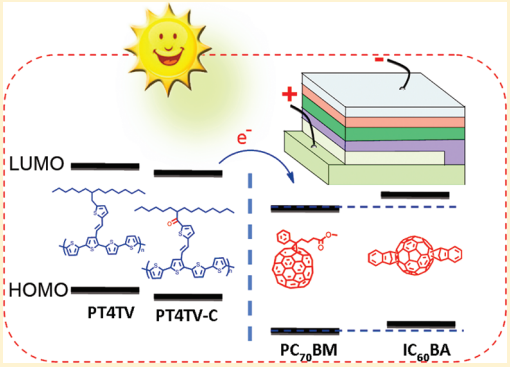

1. INTRODUCTION

Bulk heterojunction (BHJ) polymer solar cells (PSCs) based on *p*-type conjugated polymers[1] as donor and *n*-type fullerene derivatives[2] as acceptor have been intensively studied in recent years for the generation of affordable, clean, and renewable energy. Advantages of the BHJ PSCs include low-cost fabrication of large-area devices, lightweight, mechanical flexibility, and easy tunability of chemical properties of the photovoltaic materials.

Polythiophene derivatives (PTs) are among the most extensively investigated conjugated polymers due to their high charge carrier mobility, strong absorption in visible region and synthetic accessibility.[3−6] Soluble poly(3-alkylthiophene)s, especially regioregular poly(3-hexylthiophene) (P3HT), are the most important semiconducting polymers for the applications in polymer solar cells (PSCs). However, the power conversion efficiency (PCE) of the PSCs based on P3HT as donor and PCBM as acceptor is limited at 4−5%,[7] because of its relatively large band gap and its high HOMO (the highest occupied molecular orbital) energy level, which result in limited light absorption and a low open circuit voltage (V_{oc}) of the PSCs.

For broadening the absorption of the PTs, the polythiophene derivatives with conjugated side chain (CSC-PTs) were designed and synthesized in our group.[8−10] The CSC-PTs possess higher hole mobility thanks to the 2-D conjugation structure, and broad absorption deriving from both the main chains and conjugated side chains, thus this family of CSC-PTs demonstrated good device performances in PSCs and organic field−effect transistors (OFETs). However, due to asymmetric nature and high concentration of the substituents employed, the as-synthesized polymers showed poorer regioregularity in terms of the direction of the concentrated alkyl chains and/or conjugated side chains projecting from the thiophene main chains. The regiorandom structure can cause a nonplanar orientation of the thiophene backbone, which is detrimental for the close packing of polymer chains in the solid state, as clearly evidenced for the featureless absorption along with the low absorption intensity of $\pi-\pi^*$ absorption.[8−10] To overcome this problem, we recently proposed a "side-chain-isolation" concept for the PTs and synthesized a CSC-PT of **PT5TPA** with styryl−triphenylamine (TPA) side chain and unsubstituted tetrathienyl spacer. **PT5TPA** showed improved planarity of the polymer backbone with red-shifted and enhanced absorption.[11] Considering the diverse molecular engineering approaches under this side chain isolated polythiophenes, such as changing the nature of side chain and spacer as well as introducing the

Received: December 6, 2011
Revised: February 17, 2012
Published: February 29, 2012

dx.doi.org/10.1021/ma2026463 | *Macromolecules* 2012, 45, 2312−2320

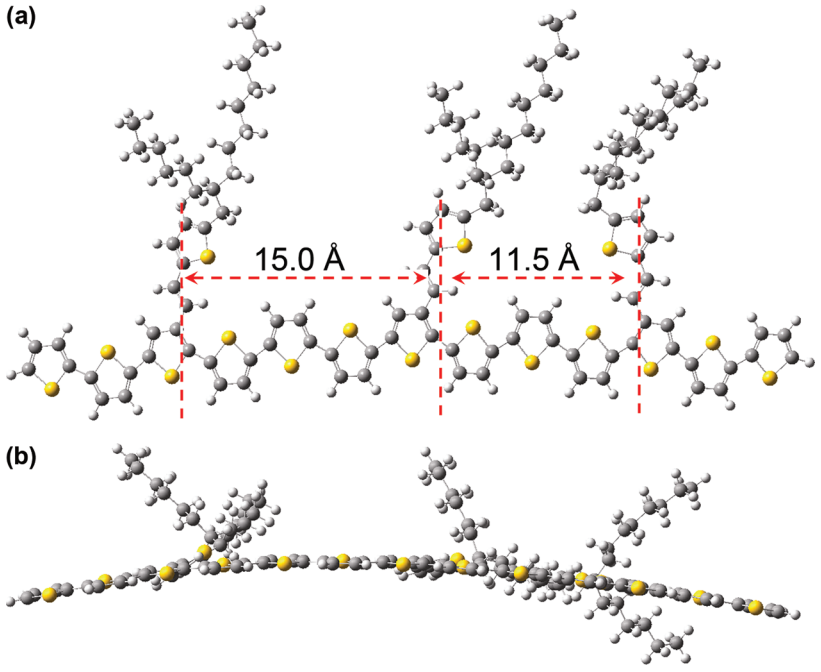

Figure 1. Optimized geometry of PT4TV: (a) top view and (b) side view.

Scheme 1. Synthetic Routs of PT4TV and PT4TV-C

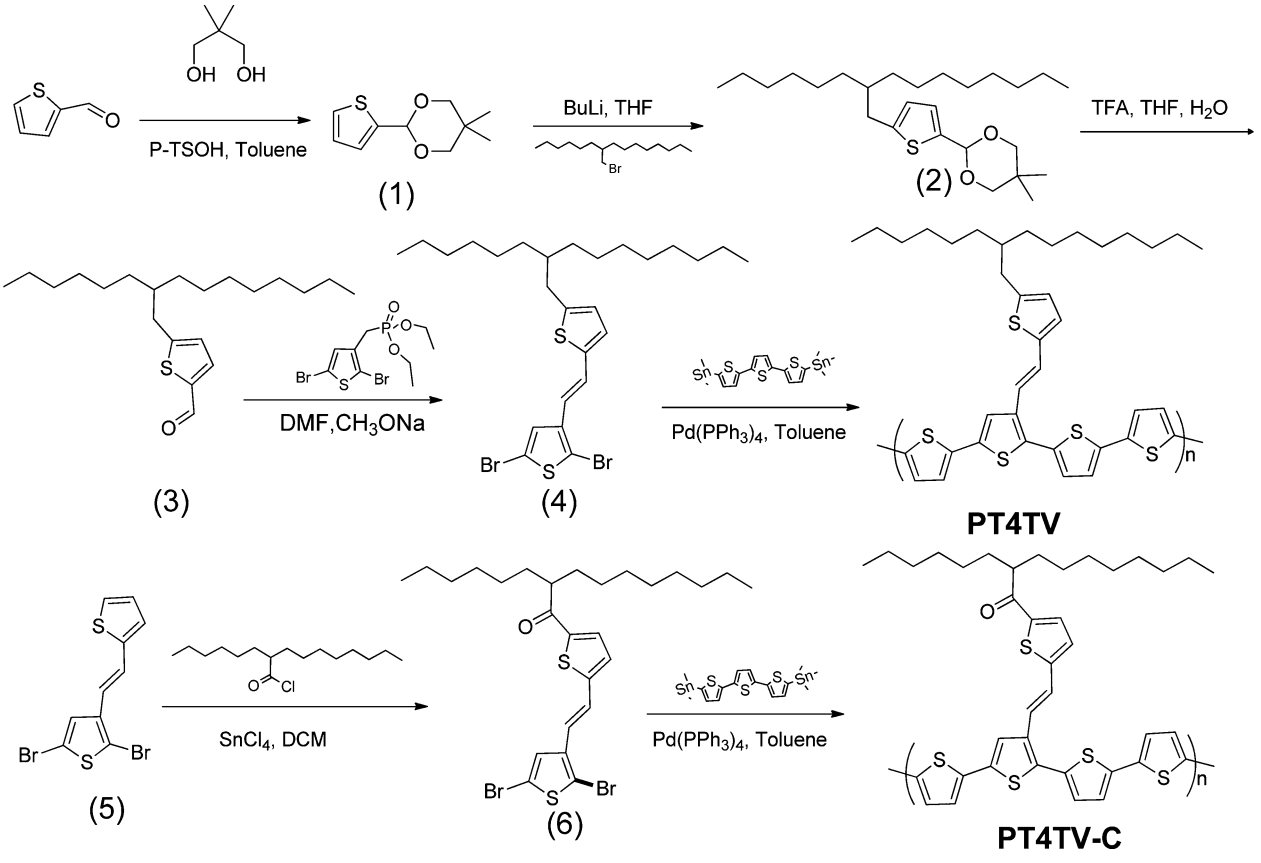

donor–acceptor (D–A) concept, CSC-PTs could open a new way for developing high performance polymer semiconductors.

Here, we designed and synthesized two new conjugated side chain isolated PTs **PT4TV** with conjugated thienylene vinylene (TV) side chain and **PT4TV-C** with the TV side chain attaching the electron-withdrawing carbonyl group. In these polymer systems, the synthesis methodology and the structure optimization were further explored. The two polymers show red-shifted and enhanced absorption of polymer backbone. The PSC based on **PT4TV** as donor and indene–C_{60} bisadduct (ICBA) as acceptor exhibited a power conversion efficiency of 3.05% with a high open circuit voltage of 0.93 V, under the

dx.doi.org/10.1021/ma2026463 | *Macromolecules* 2012, 45, 2312–2320

Scheme 2. Synthetic Routs of Reference Polymers of PT3TV and PT3TV-C

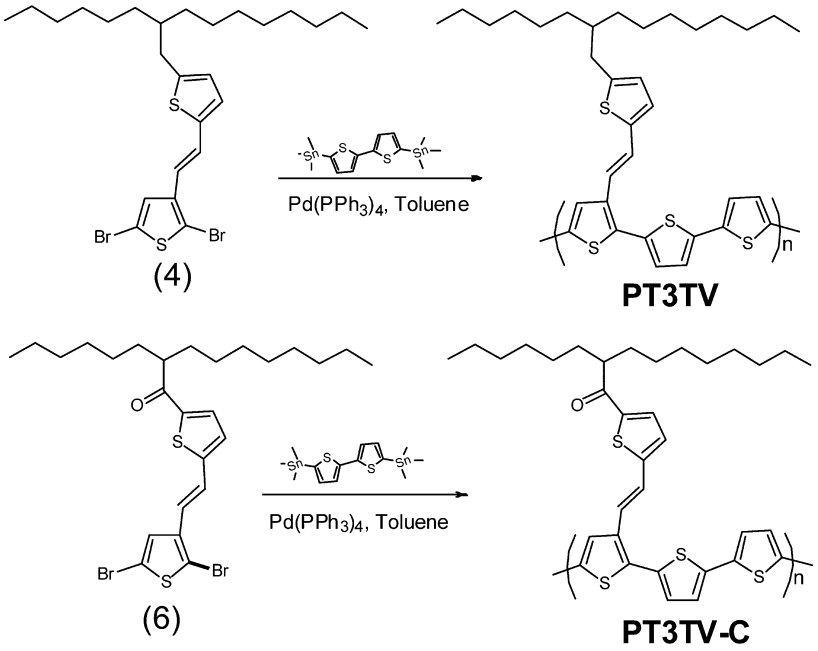

illumination of AM1.5G, 100 mW/cm^2. These results demonstrated a promising future for such types of polymers.

2. RESULTS AND DISCUSSION

Polymer Design and Side Chain Engineering. The molecular conformations of **PT4TV** and its polymer analogue of **PT3TV** (for comparison) were investigated by molecular mechanics simulation with COMPASS force field within the materials studio package.[12] As shown in Figure 1, in the proposed molecular structure of the conjugated side-chain-isolated **PT4TV**, the side−chains oriented in the tail-to-tail directions in the extended polymer conformation are spaced approximately 11.5 Å apart while those side chains orientated in the head-to-tail fashions are 15.0 Å apart. For the polymer analogue with bithienyl spacer (**PT3TV**), the optimized geometry is shown in Figure S1 in the Supporting Information. This shortening in the thiophene spacer brought a tail-to-tail side chains orientation distance of 9.5 Å and aroused clear twisting of the backbone, due to steric hindrance of the large side chains with each other. Thus, this side chain isolation approach combines the asymmetric thiophene units with conjugated side chains and the unsubstituted trithienyl spacers to minimize the steric interactions between the neighboring side chains, hence preserving backbone planarity.

Compared to our recently developed side chain isolated PT5TPA,[11] the replacing of the twisted propeller TPA side chain with planar thiophene side chain is aimed at promoting the planarity of the whole backbone and thus denser packing of the polymer chains in the solid. Another benefit of replacing TPA with the thiophene unit is brought by the shorter side chain width of thiophene (2.6 Å) unit relative to that of bulky TPA (7.1 Å). Consequently, the side chain isolated spacer can be shortened from four thiophene units (in PT5TPA)[11] to three units (in **PT4TV** and **PT4TV-C**). In synthesis methodology, this change in thiophene spacer can overcome the tedious synthetic approach used in developing PT5TPA for easy realization of the side chain isolation concept.

In addition, appending electron-deficient group at the terminal of the conjugated side chain can lower the HOMO energy level and narrow the band gap of the side-chain-conjugated polymers.[13,14] Therefore, we designed and synthesized **PT4TV-C** with an additional electron-withdrawing carbonyl group attaching to the TV conjugated side chain. Thus, the as-presented synthesis strategy allows direct comparison of polymers with the same polymer backbone and conjugated side chains but different functional groups on the side chain for elucidating their structure−property relationships.

Polymer Synthesis and Characterization. Chemical structures and synthetic routes of **PT4TV** and **PT4TV-C** are depicted in Scheme 1. Initially, thiophen-2-carbaldehyde was protected by reacting with 2,2-dimethyl-1,3-propandiol under acidic conditions, yielding the acetal **1**. The alkylation of acetal **1** was performed by lithiation with *n*-butyllithium followed by quenching with alkyl bromide, giving acetal derivative **2**. The acetal derivative **2** was converted into its corresponding aldehyde **3** by dedioxanylation with trifluoroacetic acid (TFA). Coupling reaction of carbaldehyde **3** with phosphonate precursor under Horner−Emmons−Wittig reaction led to the dibrominated monomer.[15] The conformation of the vinylic bonds of monomer **4** have unequivocally been designated as E on the basis of J_{HH} vinylic coupling constant (ca. 16 Hz). In contract to Monomer **4**, acylated thiophene monomer **6** is more easily accessible via the Friedel−Crafts acylation of compound **5** with 2-hexyldecanoyl chloride and $SnCl_4$. The two polymers, **PT4TV** and **PT4TV-C** were successfully synthesized by Stille coupling reaction[16] of the distannyl trithiophene and dibromo compounds (**4** or **6**). The two polymers have good solubility in chlorinated solvents, such as dichlomathane, chloroform and dichlorobenzene, which is important for their application in PSCs. The chemical structures of **PT4TV** and **PT4TV-C** were confirmed by ^{1}H NMR spectra and Fourier transform infrared (FT-IR) absorption spectroscopy. In the ^{1}H NMR spectra (see Figure S2 in the Supporting Information), the ratios of integrated peak areas of olefinic to aliphatic

dx.doi.org/10.1021/ma2026463 | Macromolecules 2012, 45, 2312−2320

protons are consistent with the proposed structures. And the appearance of carbonyl group in **PT4TV-C** is clearly supported by characteristic C=O stretching vibrations at 1648 cm^{-1} in the FT-IR spectra (see Figure S3 in the Supporting Information). For the reference polymers with bithienyl spacer (**PT3TV** and **PT3TV−C**), the synthetic routs are depicted in Scheme 2 and the details of synthesis were provided in the Supporting Information.

Thermal Stability. Thermal stability of the polymers was investigated with thermogravimetric analysis (TGA), as shown in Figure S4 in the Supporting Information. The TGA analysis reveals that the onset temperatures with 5% weight loss (T_d) of **PT4TV** and **PT4TV-C** are 394 and 374 °C, respectively (see Table 1). This indicates that the polymers are stable enough for the applications in optoelectronic devices.

Table 1. Thermal, Optical and Electrochemical Properties of the Polymers

polymers	T_d[a] (°C)	λ_{max}[b] (nm)	λ_{edg}[c] (nm)	E_g^{opt} (eV)	HOMO (eV)	LUMO (eV)	E_g^{ec}[d] (eV)
P3HT	–	550	650	1.91	−4.90	−2.80	2.10
PT4TV	394	372, 557	663	1.87	−5.21	−3.15	2.06
PT4TV-C	374	378, 561	680	1.82	−5.26	−3.35	1.91

[a]5% weight loss temperature measured by TGA under N_2. [b]Film absorption maximum. [c]Film absorption edge. [d]Estimated using the equations $E_g^{ec} = E_{LUMO}^{ec} - E_{HOMO}^{ec}$

Optical Properties. Figure 2 shows the absorption spectra of **PT4TV and PT4TV-C** solution in chloroform and film on quartz plate, along with the absorption spectra of reference polymers of **PT3TV** and **PT3TV-C** with concentrated side chains for comparison. The molar extinction coefficients per repeating unit of **PT4TV** at peak wavelength is 3.43 × 10^4 M^{-1} cm^{-1}, higher than that of **PT4TV-C** (3.20 × 10^4 M^{-1} cm^{-1}). The solution and film absorptions of **PT4TV** and **PT4TV-C** display similar broad absorption band with two distinct absorption peaks and steep absorption edges. The weak absorption peaks around 400 nm originate from the absorption of the conjugated side chain, while the maximum absorptions of **PT4TV** and **PT4TV-C** at 580 nm correspond to the $\pi-\pi^*$ transition of the polymer backbone. Thus, both the main chain and side chain contribute to the broad nature of the absorption spectra of the polymers, which is a common feature for the PTs with conjugated side chains.[8,9] Because of an enlarged π-system, the film absorption of **PT4TV** is red-shifted by ca. 10 nm than that of **P3HT**, while for that of **PT4TV-C**, more pronounced red-shift by ca. 20 nm was recorded largely brought by additional charge transfer effect between polymer main chain and pendant carbonyl group. Thus, the absorption edges of the polymer film reached 663 nm for **PT4TV** and 680 nm for **PT4TV-C**, corresponding to respective optical band gap of 1.87 and 1.82 eV (see Table 1). Owing to improved planarity of the polymer main chain and denser packing of side chains, the absorption spectra of the two polymers are red-shifted relative to that (658 nm) of their polymer analogue of **PT5TPA** with propeller TPA side chain.[11] Furthermore, shoulder peak at ca. 620 nm, especially for **PT4TV**, appears in the absorption spectra of the polymer solutions and films, indicative of aggregated polymer chains in both states. As shown in Figure 2a, when the polymer solution was heated to 80 °C, the absorption peaks blue shift, and the shoulder peak at ca. 600 nm weakened, reflecting partial disaggregation of the polymer backbone at high temperature. For the control polymers (**PT3TV** and **PT3TV-C**), both solution and film absorptions demonstrated blue-shifted and featureless absorptions with decreased absorption intensity of $\pi-\pi^*$ transition due to the nonplanarity conformation. These results further highlighted the importance of the side chain isolation approach in developing two-dimensional conjugated polymers.

Electrochemical Properties. The highest occupied molecular orbital (HOMO) and the lowest unoccupied molecular orbital (LUMO) energy levels of the conjugated polymers are important parameters in determining the V_{oc} and excitons dissociation efficiency in PSCs, and they can be measured from the onset oxidation potential (φ_{ox}) and onset reduction potential (φ_{red}) of cyclic voltammograms of the polymers according to the following equations:[17] $E_{HOMO} = -e(\varphi_{ox} + 4.71)$ (eV) and $E_{LUMO} = -e(\varphi_{red} + 4.71)$, where the unit of potential is V vs. Ag/Ag^+.

Figure 3 shows the cyclic voltammograms of the two copolymers. The onset reduction potential (φ_{red}) and onset oxidation potential (φ_{ox}) of **PT4TV** are −1.55 and +0.50 V vs Ag/Ag^+, respectively, corresponding to LUMO and HOMO energy levels of −3.16 and −5.21 eV, respectively. After introducing the electron deficient carbonyl group in **PT4TV-C**, its LUMO energy level is decreased to −3.35 eV and its HOMO energy level is down-shifted to −5.26 eV, leading to a reduced electrochemical bandgap (E_g^{ec}) of 1.91 eV for **PT4TV-C**. The electronic energy levels and electrochemical bandgaps of the two polymers along with that of P3HT were also listed in

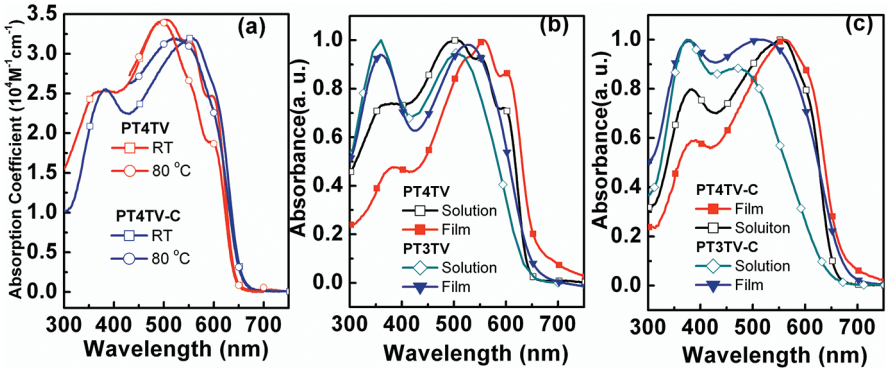

Figure 2. (a) Solution absorption spectra of **PT4TV** and **PT4TV-C** at room temperature and at 80 °C; (b) Solution and film absorption spectra of **PT4TV** and **PT3TV**; (c) Solution and film absorption spectra of **PT4TV-C** and **PT3TV-C**.

dx.doi.org/10.1021/ma2026463 | *Macromolecules* 2012, 45, 2312−2320

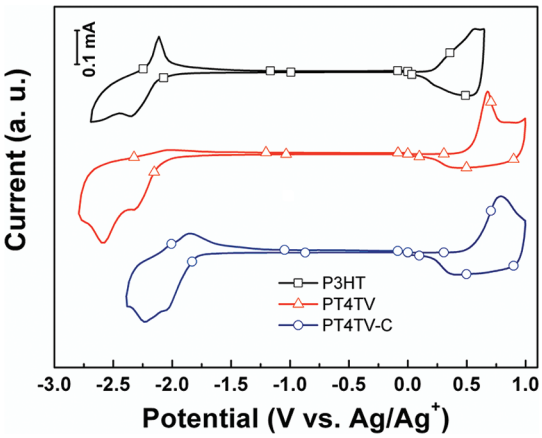

Figure 3. Cyclic voltammograms of **PT4TV** and **PT4TV-C** films on a Pt electrode measured in 0.1 mol L^{-1} Bu_4NPF_6 acetonitrile solutions at a scan rate of 100 mV s^{-1}.

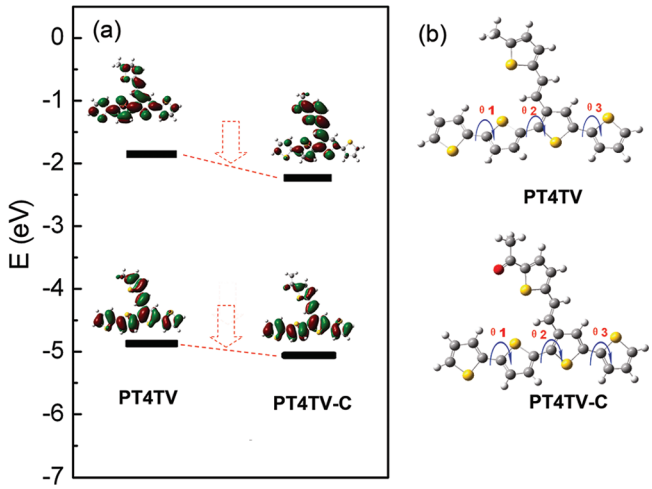

Figure 4. (a) HOMO and LUMO energy levels (eV) and the frontier molecular orbitals obtained from DFT calculations on **PT4TV** and **PT4TV-C** with a chain length n = 1 at B3LYP/6-31G* level of theory along with (b) optimized geometry.

Table 1 for clear comparison. For both polymers, the lower HOMO energy level relative to P3HT can provide better air stability in ambient conditions and higher open circuit voltage (V_{oc}) of the PSCs because the V_{oc} is usually proportional to the difference between the LUMO level of the acceptor and the HOMO level of the donor.[6]

X-ray Diffraction and Hole Mobility. As shown in Figure S5 in the Supporting Information, X-ray diffraction patterns of the pristine polymer films exhibit (100) diffraction peaks at 2θ = 3.42° and 3.20°, respectively, corresponding to an interchain d-spacing of 25.82 Å for **PT4TV** and 27.60 Å for **PT4TV-C**. These values are larger than that of P3HT (16.4 Å)[7a] due to the bulky side chain incorporated. However, the (010) diffraction peaks are not observed for the two polymers.

Hole mobility of the two polymers was measured by space charge limit current (SCLC) method, as shown in Figure S6 in Supporting Information. **PT4TV** demonstrated a hole mobility of 4.08×10^{-3} cm^2 V^{-1} s^{-1}, which is four times higher than that (9.5×10^{-4} cm^2 V^{-1} s^{-1}) of **PT4TV-C**. Notably, the hole mobility of **PT4TV** is also higher than that of our previously developed side chain isolated PT5TPA,[11] and the improved planarity of **PT4TV** can account for this phenomenon.

Theoretical Calculations. To provide further insight into the fundamentals of molecular architecture, molecular simulation was carried out for **PT4TV** and **PT4TV-C**, with a chain length of n = 1 at the DFT B3LYP/6-31G(d) level with the Gaussian 03 program package.[18] The bulky alkyl chain was replaced with methyl group in the calculation to avoid excessive computation demand, since they do not significantly affect the equilibrium geometry and thus the electronic properties. All C=C bonds outside the aromatic rings were set to be in trans configuration.

As depicted in Figure 4a, for **PT4TV**, there is a significant overlap between the HOMO and LUMO. However, for **PT4T-C**, the electron density distributions at LUMO become slightly localized near the electron-withdrawing carbonyl groups, and the well-separated distribution of HOMO and LUMO energy levels indicate that a transition between them can be considered to be a charge-transfer transition.[13] As a result, both the HOMO and LUMO energy level as well as the bandgap are decreased.

The optimized geometries are shown in Figure 4b, and relevant dihedral angles are listed in Table 2. Notably, the appearance of ICT interaction in **PT4TV-C** also aroused

Table 2. Calculated Dihedral Angles of Polymers

	dihedral angle (deg)			
polymers	$\theta 1$	$\theta 2$	$\theta 3$	θ^a
PT4TV	16.84	35.08	19.35	71.27
PT4TV-C	19.44	34.83	19.16	73.43

[a]The dihedral angle of the entire unit, $\theta = \theta 1 + \theta 2 + \theta 3$.

increased dihedral angles along the backbone, which is detrimental for the planarity of the backbone and close packing of polymer chains in the solid state. Similar phenomena were also observed in conjugated polymers with pendant acceptors.[13,14] And the calculated results can partly explain the better hole mobility of **PT4TV** relative to that of **PT4TV-C**.

In addition, it can be seen from Figure 4 and Table 1 that although discrepancies exist between the calculation and experimental results, the trends of variation in the HOMO and LUMO energy levels, as well as the energy gaps, are consistent.

Photovoltaic Properties. The photovoltaic properties of **PT4TV and PT4TV−C** (Table 3) were studied by fabricating the bulk heterojunction PSCs with the device configuration of ITO/PEDOT: PSS/polymer: acceptors/Ca/Al. Here, two different fullerene derivatives $PC_{70}BM$ and $IC_{60}BA$ were used as acceptor in the PSCs. The molecular structures and the electronic energy level diagrams of the donor and acceptor materials were displayed in Figure 5. Figure 6 shows the $J-V$ curves of the PSCs based on **PT4TV** or **PT4TV-C** as donor and $PC_{70}BM$ or $IC_{60}BA$ as acceptor under the illumination of AM 1.5, 100 mW·cm^{-2}.

With the widely used $PC_{70}BM$ as acceptor, the PSC based on PT4TV showed a moderate PCE of 2.80% along with a V_{oc} of 0.67 V and a FF of 51.1%. The FF value is significantly improved in comparison with the PTs with concentrated side chains. For example, FF values of the PSCs based on the concentrated side chain CSC-PTs, PT-1,[8a] and PT-2[8d] (their molecular structures are shown in Scheme 1 in Supporting Information) were only 43% and 38% respectively. The higher FF of the **PT4TV**-based PSCs could be related to the closely packing of the polymer main chains in this side-chain-isolated PTs and its higher hole mobility. The appending of carbonyl

dx.doi.org/10.1021/ma2026463 | Macromolecules 2012, 45, 2312−2320

Table 3. Photovoltaic Parameters of PSCs Based on Fullerene Acceptor of $PC_{70}BM$, $IC_{60}BA$

polymers	acceptors	ratio[a]	V_{oc} (V)	J_{sc} (mAcm^{-2})	FF (%)	PCE (%)	thickness (nm)
PT4TV	$PC_{70}BM$	1:1	0.67	7.59	55.1	2.80	78
	$IC_{60}BA$	1:0.8	0.93	5.83	56.2	3.05	75
PT4TV-C	$PC_{70}BM$	1:1	0.74	4.48	36.4	1.21	70
	$IC_{60}BA$	1:1	1.01	3.78	36.8	1.41	75

[a]Polymer/fullerene weight ratio.

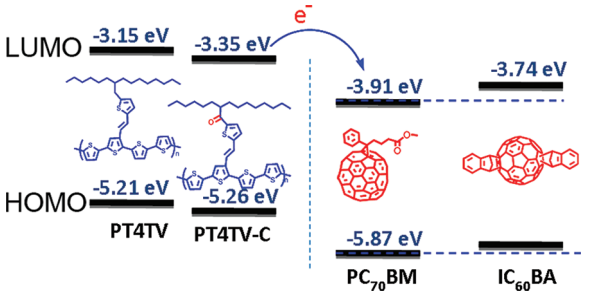

Figure 5. Energy level diagrams for polymer donor of PT4TV and PT4TV−C along with acceptors of $PC_{70}BM$ and $IC_{60}BA$.

group in **PT4TV-C** produced a higher V_{oc} of 0.74 V, 0.07 V higher than that of the **PT4TV**-based device due to its lower lying HOMO energy level. But due to a lower hole mobility, the PSC based on **PT4TV-C** showed a lower J_{sc} of 4.48 mAcm^{-2} and a lower FF of 36.4%, which result in an overall lower efficiency of 1.21%.

To further improve the efficiency, it is important to use fullerene acceptors with higher LUMO energy to increase V_{oc}. Along this line, an indene−C_{60} bisadduct (ICBA)[2] developed in our group with a higher LUMO energy level of −3.74 eV was incorporated in further device optimization. As a result, a higher V_{oc} of 0.93 V for **PT4TV** and 1.01 V for **PT4TV-C** were obtained. Although $IC_{60}BA$−based devices generate smaller J_{sc} values than those of $PC_{70}BM$ devices, presumably as a result of lower molar extinction coefficients of $IC_{60}BA$ relative to that of $PC_{70}BM$, improved PCE of 3.05% for **PT4TV** and 1.41% for **PT4TV-C** was still achieved because the increased V_{oc} partially compensates the decreased J_{sc} value. The J_{sc} values of the PSCs were confirmed by the IPCE results as shown in Figures 6, parts b and d.

Morphology. The morphologies of the blend films were investigated by atomic force microscopy (AFM). As shown in Figure S7 in Supporting Information, the blend films demonstrated different phase separation state with root-mean-square (rms) roughness of 2.16 nm for **PT4TV**/$PC_{70}BM$ composite film, 9.62 nm for **PT4TV**/$IC_{60}BA$ composite film, 1.39 nm for **PT4TV-C**/$PC_{70}BM$ composite film and 1.36 nm for **PT4TV-C**/$IC_{60}BA$ composite film, indicating different miscibility between the copolymers and fullerene derivatives. The large domain size for **PT4TV**/$IC_{60}BA$ composite film suggested that even better device performance can be expected by further device engineering, such as thermal annealing, solvent annealing, and additives to promote proper phase separation.

3. CONCLUSION

Two new conjugated side chain isolated PTs with thienylene−vinylene (TV) conjugated side chain and unsubstituted trithienyl spacer, **PT4TV** and **PT4TV-C**, were designed and

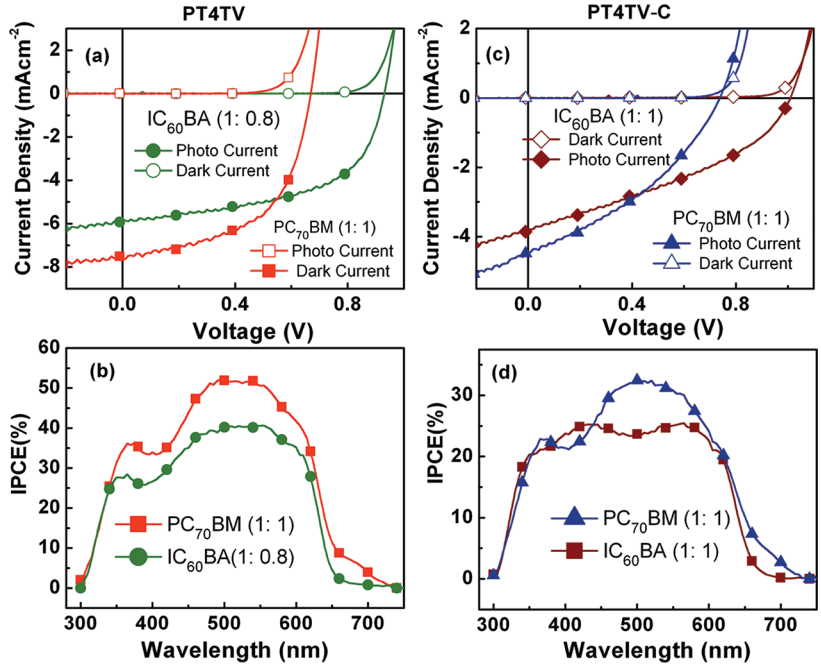

Figure 6. Current density−voltage curves of PSCs based on composite films of (a) **PT4TV**−fullerenes and (c) **PT4TV-C**−fullerenes under the illumination of AM 1.5, 100 mW·cm^{-2}. Incident-photon-to-converted-current efficiency (IPCE) spectra of the corresponding devices: (b) **PT4TV**−fullerenes and (d) **PT4TV-C**−fullerenes.

dx.doi.org/10.1021/ma2026463 | *Macromolecules* 2012, 45, 2312−2320

synthesized. In comparison with PT4TV, PT4TV-C possesses an additional electron-withdrawing group attaching to the TV side chain. **PT4TV** showed lower HOMO energy levels at −5.21 eV, higher hole mobility of 4.08×10^{-3} cm^2 V^{-1} s^{-1}, and red-shifted and enhanced absorption with steep absorption edge at 663 nm. **PT4TV-C** possessed further down-shifted HOMO level at −5.26 eV and red-shifted absorption band with absorption edge at 680 nm due to the electron-withdrawing carbonyl group on its side chain, but lower hole mobility due to the poorer planarity of the polymer. The PSC based on **PT4TV** as donor and $IC_{60}BA$ as acceptor displayed a power conversion efficiency of 3.05% with a high V_{oc} of 0.93 V, under the illumination of AM1.5G, 100 mW/cm^2.

4. EXPERIMENTAL SECTION

4.1. Instrumentation. ^{1}H NMR spectra and ^{13}C NMR spectra were measured on a Bruker DMX−400 spectrometer with *d*-chloroform as the solvent and trimethylsilane as the internal reference. UV−visible absorption spectra were measured on a Hitachi U-3010 UV−vis spectrophotometer. Mass spectra were recorded on a Shimadzu spectrometer. Elemental analyses were carried out on a flash EA 1112 elemental analyzer. Thermogravimetric analysis (TGA) was conducted on a Perkin−Elmer TGA−7 thermogravimetric analyzer at a heating rate of 20 °C/min and under a nitrogen flow rate of 100 mL/min. Molecular weight of the polymer was measured by Gel permeation chromatography (GPC), using polystyrene as standard and THF as the eluent. The electrochemical cyclic voltammetry was performed on a Zahner IM6e Electrochemical Workstation, in an acetonitrile solution of 0.1 mol/L tributylammonium hexafluorophosphate (*n*-Bu_4NPF_6) at a potential scan rate of 100 mV/s with an Ag/Ag^+ reference electrode and a platinum wire counter electrode. Polymer film was formed by drop-casting 1.0 mL of polymer solutions in THF (analytical reagent, 1 mg/mL) onto the glassy carbon working electrode, and then dried in the air. The film morphology was measured using an atomic force microscope (AFM, SPA-400) using the tapping mode.

4.2. Photovoltaic Device Fabrication and Characterization. The PSCs were fabricated with a configuration of ITO/PEDOT:PSS (40 nm)/active layer (ca. 70−80 nm)/ Ca(20 nm)/Al(80 nm). A thin layer of PEDOT:PSS (poly(3,4-ethylenedioxythiophene): poly(styrenesulfonate)) was spin-cast on precleaned ITO-coated glass from a PEDOT:PSS aqueous solution (Baytron P VP AI 4083 from H. C. Starck) at 2000 rpm and dried subsequently at 150 °C for 30 min in air, then the device was transferred to a glovebox, where the active layer of the blend of the polymer and fullerene derivatives was spin-coated onto the PEDOT:PSS layer. Finally, a Ca/Al metal top electrode was deposited in vacuum onto the active layer at a pressure of ca. 5×10^{-5} Pa. The active area of the device was ca. 4 mm^2.

The thickness of the active layer was determined by an Ambios Tech. XP-2 profilometer. The current density−voltage (J−V) characteristics were measured on a computer−controlled Keithley 236 Source−Measure Unit. A xenon lamp coupled with AM 1.5 solar spectrum filter was used as the light source, and the optical power at the sample was 100 mW/cm^2. The hole mobility was calculated by fitting the dark J-V curves for the hole-only devices to SCLC model at low voltages, in which the current density is given by $J = 9\varepsilon_0\varepsilon_r\mu V^2/8L^3\exp[0.891\gamma(V/L)^{0.5}]$, where $\varepsilon_0\varepsilon_r$ represents the permittivity of the material, μ is the mobility, γ is the field activation factor, and L the thickness of the active layer. The applied bias voltage is corrected for the built-in potential so that $V = V_{applied} - V_{bi}$. Thin-film X-ray diffraction (XRD) was recorded on a Bruker D8 Discover thin-film diffractometer with Cu Kα radiation (λ = 1.540 56 Å) operated at 40 keV and 40 mA.

4.3. Materials. Diethyl (2,5-dibromothiophen-3-yl) methylphosphonate,[8] 5,5″-Bis(trimethylstannyl)-2,2′:5′,2″-terthiophene[19] were prepared according to the method reported in literatures. Tris(triphenylphosphine)palladium, *N*-bromosuccinimide, and benzoyl peroxide were purchased from Sigma-Aldrich Chemical Co. P3HT with regioregularity of 90%-94% was purchased from Rieke Metals Inc.

4.4. Synthesis of the Polymers. The synthetic routes of the polymers are shown in Scheme 1. The detailed synthetic processes of the monomers and polymers are described in the following.

*5,5-Dimethyl-2-(thiophen-2-yl)-1,3-dioxane (**1**).* To 200 mL of a three-necked flask attached with a Dean−Stark trap condenser were added thiophen-2-carbaldehyde (22.4 g, 200 mmol), 2,3-dimethylbutane-2,3-diol (31.2 g, 300 mmol), *p*-TsOH (1.92 g, 10 mmol), and toluene (120 mL) under N_2.The mixture was refluxed by stirring overnight and was neutralized with saturated $NaHCO_3$ aqueous solution. The organic layer was extracted with ether, dried over anhydrous Na_2SO_4, and evaporated to dryness. The residue was purified by Al_2O_3 column chromatography to afford the title compound (**1**) (18 g, 50.0%). GC−MS: m/z = 180. ^{1}H NMR (400 MHz, $CDCl_3$, δ, ppm): 7.30 (d, J = 4.8 Hz, 1H), 7.05−7.04 (m, 5H, ArH), 6.99 (d, J = 4 Hz, 2H, ArH), 7.14 (d, J = 3.4 Hz, 1H), 7.00−6.98 (m, 1H), 5.65 (s, 1H), 3.76 (d, J = 11.5 Hz, 2H), 3.64 (d, J = 10.9 Hz, 2H), 1.29 (t, J = 6.4 Hz, 3H), 0.80 (t, J = 6.4 Hz, 3H). Anal. Calcd for $C_{10}H_{14}O_2S$: C, 60.57; H, 7.12; S, 16.17. Found: C, 60.49; H, 7.02; S: 16.25.

*2-(5-(2-Hexyldecyl)thiophen-2-yl)-5,5-dimethyl-1,3-dioxane (**2**).* Compound **1** (10.8 g, 60 mmol) was dissolved in 300 mL of dry THF in a three−neck flask. The flask was filled with nitrogen and cooled to −78 °C. A solution of *n*-butyllithium in *n*-hexane (2 mol L^{-1}, 15 mL) was added dropwise to the flask using a glass injector through a septum cap. The solution was stirred at −78 °C for 1 h. Then, 1-bromo-2-hexyldecane (18.3 g, 60 mmol) was dissolved in 50 mL of dry THF and added to the solution. The solution was stirred at RT overnight, then 300 mL of saturated NH_4Cl aq. was added to the solution and the product was extracted with ethyl acetate. The ethyl acetate solution was dried with Na_2SO_4, and the solvent was evaporated. The product was purified by column chromatography on silica−gel to yield a slightly yellow oil of 21.1 g (yield: 83.3%). GC−MS: m/z = 422. ^{1}H NMR (400 MHz, $CDCl_3$, δ, ppm): 6.90 (d, J = 3.2 Hz, 1H), 6.60 (d, J = 3.2 Hz, 1H), 5.55 (s, 1H), 3.74 (d, J = 11.5 Hz, 2H), 3.48 (d, J = 10.9 Hz, 2H), 2.68 (d, J = 6 Hz, 2H), 1.58 (s, 1H), 1.26−1.23 (m, 24H), 1.00−0.80 (m, 12H). Anal. Calcd for $C_{26}H_{46}O_2S$: C, 73.88; H, 10.97; S, 7.59. Found: C, 74.01; H, 11.05; S: 7.45.

*5-(2-Hexyldecyl)thiophene-2-carbaldehyde (**3**).* THF (30 mL) and water (30 mL) were added to a flask containing acetal **2** (18.9 g, 45 mmol) and TFA (10 mL). The resulting reaction mixture was refluxed for overnight, quenched with saturated aqueous sodium bicarbonate, and extracted with dichloromethane. The combined organic phases were washed with aqueous sodium bicarbonate, dried over anhydrous Na_2SO_4, and evaporated in vacuo. The pure product **3** was obtained by silica gel chromatography using a mixture of methylene chloride and *n*-hexane (1:10) as an eluent to yield an oil of 13.44 g(yield 95%). GC−MS: m/z = 336. ^{1}H NMR (400 MHz, $CDCl_3$, δ, ppm): 9.80 (s, 1H), 7.58 (d, J = 3.6 Hz, 1H), 6.85 (d, J = 3.6 Hz, 1H), 2.68 (d, J = 6 Hz, 2H), 1.58 (s, 1H), 1.26−1.23 (m, 24H), 0.80 (m, 6H). Anal. Calcd for $C_{21}H_{36}OS$: C, 74.94; H, 10.78; S, 9.53. Found: C, 74.85; H, 10.89; S: 9.68.

*(E)-2,5-Dibromo-3-(2-(5-(2-hexyldecyl)thiophen-2-yl)vinyl)-thiophene. (**4**).* Under an ice−water bath, diethyl (2,5-dibromothiophen-3-yl) methylphosphonate (1.38 g, 5 mmol) and aldehyde **3** (2.01 g, 6 mmol) were dissolved in 30 mL of DMF, and then CH_3ONa (0.6 g, 11 mmol) in 10 mL of DMF was added dropwise to the solution. After reaction for 2 h at room temperature, 300 mL of saturated NH_4Cl(aq) was added to the solution and the product was extracted with ethyl acetate. The ethyl acetate solution was dried with Na_2SO_4, and the solvent was evaporated. The product was purified by column chromatography on silica gel to yield a yellow oil of 1.77 g (yield: 60.0%). ^{1}H NMR (400 MHz, $CDCl_3$, δ, ppm): 7.13 (s, 1H), 6.95 (d, J = 15 Hz, 1H), 6.87 (d, J = 3.5 Hz, 1H), 6.70 (d, J = 15 Hz, 1H), 6.40 (d, J = 3.5 Hz, 1H), 7.47 (m, 4H), 2.72 (d, J = 6.7 Hz, 1H), 1.65 (s, 1H), 1.28−1.27 (br, 24H), 0.80 (t, J = 6.4 Hz, 6H). ^{13}C NMR (150 MHz, $CDCl_3$, δ, ppm): 146.250; 140.776; 140.077; 128.233; 128.049; 127.4101; 126.890; 125.999; 125.887; 119.774; 119.714; 119.205;

dx.doi.org/10.1021/ma2026463 | *Macromolecules* 2012, 45, 2312−2320

112.806; 110.158; 78.305; 78.093; 77.881; 61.401; 41.033; 35.929; 34.267; 34.253; 32.982; 32.946; 31.014; 30.685; 30.399; 27.647; 27.631; 23.748; 22.055; 15.258; 15.159. Anal. Calcd for $C_{26}H_{38}Br_2S_2$: C, 54.35; H, 6.67; S, 11.16. Found: C, 54.51; H, 6.71; S: 11.24.

*(E)-1-(5-(2-(2,5-Dibromothiophen−3-yl)vinyl)thiophen-2-yl)-2-hexyldecan-1-one (**6**).* $SnCl_4$ (0.336 g, 9 mmol) was added to a mixture of 2-((*E*)-2-(2,5-dibromothiophen-3-yl)vinyl)thiophene (compound **5**, 3.1 g, 6 mmol) and 2-hexyldecanoyl chloride (2.2 g, 8 mmol) in 50 mL of methylene chloride at 0 °C. After stirring at 0 °C for about 1 h, water was added, and the reaction mixture was diluted with methylene chloride. The mixture was washed successively with water and a saturated aqueous solution of $NaHCO_3$ and then dried over $MgSO_4$. Upon the removal of solvent, the dark-black residue was subjected to column chromatography on silica gel with ethyl acetate/hexane (v/v, 1:10) as the eluent, followed by recrystallization from acetate to offer a yellow solid (2.34 g, 50.0% yield). ^{1}H NMR (400 MHz, $CDCl_3$, δ, ppm): 7.59 (s, J = 3.6 Hz 1H), 7.17 (s, 1H), 7.10 (d, J = 3.6 Hz, 1H), 6.98 (s, 2H), 6.40 (d, J = 3.5 Hz, 1H), 3.15 (s, 1H), 1.76 (s, 1H), 1.58 (s, 2H), 1.28−1.27 (br, 20H), 0.80 (t, J = 6.4 Hz, 6H). ^{13}C NMR (150 MHz, $CDCl_3$, δ, ppm): 198.338; 150.638; 144.997; 139.210; 133.093; 128.239; 128.186; 124.595; 123.755; 113.380; 112.846; 49.300; 34.066; 32.859; 32.678; 30.830; 30.492; 30.427; 30.269; 28.749; 28.715; 23.668; 23.615; 15.123; 150.78. Anal. Calcd for $C_{26}H_{36}Br_2OS_2$: C, 53.06; H, 6.17; S, 10.90. Found: C, 53.12; H, 6.23; S: 10.83.

PT4TV. Under the protection of argon atmosphere, 0.5 mmol of 5,5″-bis(trimethylstannyl)-2,2′:5′,2″-terthiophene (0.287 g) was put into a two-neck flask. Then 12 mL of degassed toluene and 0.5 mmol of Monomer **4** (0.287 g) were added to the mixture. The solution was flushed with argon for 10 min, and then 25 mg of $Pd(PPh_3)_4$ was added. After another flushing with argon for 20 min, the reactant was heated to reflux for 24 h. Then the reactant was cooled to room temperature and the polymer was precipitated by adding 200 mL of methanol, filtered through a Soxhlet thimble, and then subjected to Soxhlet extraction with methanol, hexane, and chloroform. The polymer was recovered as solid from the chloroform fraction by rotary evaporation. The solid was dried under vacuum for 12 h to get **PT4TV**. The yield of the polymerization reaction was about 60%. GPC: M_n = 7.57 kg·mol^{-1}, M_w/M_n = 3.4. ^{1}H NMR (400 MHz, $CDCl_3$, δ, ppm): 7.40−7.27 (br, 4H), 7.27−7.17 (br, 7H), 2.70 (br, 1H), 1.66 (br, 1H), 1.28−1.27 (br, 24H), 0.80 (m, 6H).

PT4TV−C. The synthesis is the same as that for **PTTVC**, except that monomer **4** is replaced by monomer **6**. GPC: M_n = 23.66 kg·mol^{-1}, M_w/M_n = 3.5. ^{1}H NMR (400 MHz, $CDCl_3$, δ, ppm): 7.70−7.27 (br, 5H), 7.26−7.10 (br, 6H), 3.18 (s, 1H), 1.80 (s, 1H), 1.62 (s, 2H), 1.29−1.24 (br, 20H), 0.80 (br, 6H).

■ ASSOCIATED CONTENT

Supporting Information

Synthesis details of **PT3TV** and **PT3TV-C**, figures showing ^{1}H NMR spectra, FT-IR spectra, TGA plots, X-ray diffraction patterns, hole mobility measurement, AFM topography images of **PT4TV** and **PT4TV-C**, and optimized geometry of **PT3TV**, a scheme showing chemical structures of two polythiophene derivatives (PT-1 and PT-2) with concentrated conjugated side chains. This material is available free of charge via the Internet at http://pubs.acs.org.

■ AUTHOR INFORMATION

Corresponding Author

*E-mail: liyf@iccas.ac.cn.

Notes

The authors declare no competing financial interest.

■ ACKNOWLEDGMENTS

This work was supported by NSFC (Nos. 51103064, 50933003, and 21021091), The Ministry of Science and Technology of China and Chinese Academy of Sciences.

■ REFERENCES

(1) (a) Li, Y. F. *Acc. Chem. Res.* **2012**, DOI: 10.1021/ar2002446. (b) Chen, J.; Cao, Y. *Acc. Chem. Res.* **2009**, *42*, 1709. (c) Cheng, Y.-J.; Yang, S.-H.; Hsu, C.-S. *Chem. Rev.* **2009**, *109*, 5868.

(2) (a) He, Y. J.; Li, Y. F. *Phys. Chem. Chem. Phys.* **2011**, *13*, 1970. (b) He, Y. J.; Chen, H.-Y.; Hou, J. H.; Li, Y. F. *J. Am. Chem. Soc.* **2010**, *132*, 1377. (c) Zhao, G. J.; He, Y. J.; Li, Y. F. *Adv. Mater.* **2010**, *22*, 4355−4358. (d) He, Y. J.; Zhao, G. J.; Peng, B.; Li, Y. F. *Adv. Funct. Mater.* **2010**, *20*, 3383−3389.

(3) (a) Yu, G.; Gao, J.; Hummelen, J. C.; Wudl, F.; Heeger, A. J. *Science* **1995**, *270*, 1789. (b) Thompson, B. C.; Fréchet, J. M. J. *Angew. Chem., Int. Ed.* **2008**, *47*, 58.

(4) (a) Nagarjuna, G.; Yurt, S.; Jadhav, K. G.; Venkataraman, D. *Macromolecules* **2010**, *43*, 8045. (b) Grenier, C. R. G.; George, S. J.; Joncheray, T. J.; Meijer, E. W.; Reynolds, J. R. *J. Am. Chem. Soc.* **2007**, *129*, 10694. (c) Perepichka, I. F.; Perepichka, D. F.; Meng, H.; Wudl, F. *Adv. Mater.* **2005**, *17*, 2281. (d) Li, Y. F.; Zou, Y. P. *Adv. Mater.* **2008**, *20*, 2952.

(5) (a) Sugiyasu, K.; Song, C.; Swager, T. M. *Macromolecules* **2006**, *39*, 5598. (b) Wu, P.-T.; Xin, H.; Kim, F. S.; Ren, G.; Jenekhe, S. A. *Macromolecules* **2009**, *42*, 8817. (c) Miyanishi, S.; Tajima, K.; Hashimoto, K. *Macromolecules* **2009**, *42*, 1610. (d) Li, H.; Sundararaman, A.; Pakkirisamy, T.; Venkatasubbaiah, K.; Schödel, F.; Jäkle, , F. *Macromolecules* **2010**, *44*, 95. (e) Rieger, R.; Beckmann, D.; Pisula, W.; Kastler, M.; Müllen, K. *Macromolecules* **2010**, *43*, 6264. Liu, P.; Wu, Y.; Pan, H.; Ong, B. S.; Zhu, S. *Macromolecules* **2010**, *43*, 6368. (f) Ong, B. S.; Wu, Y.; Liu, P.; Gardner, S. *J. Am. Chem. Soc.* **2004**, *126*, 3378. (g) Ong, B. S.; Wu, Y.; Li, Y.; Liu, P.; Pan, H. *Chem.−Eur. J.* **2008**, *14*, 4766.

(6) (a) Liang, Y.; Xiao, S.; Feng, D.; Yu, L. *J. Phys. Chem. C* **2008**, *112*, 7866. (b) Thompson, B. C.; Kim, B. J.; Kavulak, D. F.; Sivula, K.; Mauldin, C.; Fréchet, J. M. J. *Macromolecules* **2007**, *40*, 7425. (c) Hou, J. H.; Chen, T. L.; Zhang, S. Q.; Huo, L. J.; Sista, S.; Yang, Y. *Macromolecules* **2009**, *42*, 9217.

(7) (a) Ma, W.; Yang, C.; Gong, X.; Lee, K.; Heeger, A. J. *Adv. Funct. Mater.* **2005**, *15*, 1617. (b) Li, G.; Shrotriya, V.; Huang, J.; Yao, Y.; Moriarty, T.; Emery, K.; Yang, Y. *Nat. Mater.* **2005**, *4*, 864.

(8) (a) Hou, J. H.; Tan, Z. A.; Yan, Y.; He, Y. J.; Yang, C. H.; Li, Y. F. *J. Am. Chem. Soc.* **2006**, *128*, 4911. (b) Hou, J. H.; Yang, C. H.; He, C.; Li, Y. F. *Chem. Commun.* **2006**, 871−873. (c) Hou, J. H.; Huo, L. J.; He, C.; Yang, C. H.; Li, Y. F. *Macromolecules* **2006**, *39*, 594−603. (d) Zhou, E. J.; Tan, Z. A.; Huo, L. J.; He, Y. J.; Yang, C. H.; Li, Y. F. *J. Phys. Chem. B.* **2006**, *110*, 26062−26067.

(9) (a) Zou, Y. P.; Sang, G. Y.; Wu, W.; Liu, Y. Q.; Li, Y. F. *Synth. Met.* **2009**, *159*, 182. (b) Wang, Y.; Zhou, E. J.; Liu, Y. Q.; Xi, H.; Ye, S.; Wu, W.; Guo, Y.; Di, C.-A.; Sun, Y. M.; Yu, G.; Li, Y. F. *Chem. Mater.* **2007**, *19*, 3361. (c) Zou, Y. P.; Wu, W.; Sang, G. Y.; Yang, Y.; Liu, Y. Q.; Li, Y. F. *Macromolecules* **2007**, *40*, 7231−7237.

(10) (a) Wagner, K.; Crowe, L. L.; Wagner, P.; Gambhir, S.; Partridge, A. C.; Earles, J. C.; Clarke, T. M.; Gordon, K. C.; Officer, D. L. *Macromolecules* **2010**, *43*, 3817. (b) Wang, H.-J.; Chan, L.-H.; Chen, C.-P.; Lin, S.-L.; Lee, R.-H.; Jeng, R.-J. *Polymer* **2011**, *52*, 326. (c) Saini, G.; Jacob, J. *Polym. Int.* **2011**, *60*, 1010. (d) Park, J. W.; Lee, D. H.; Chung, D. S.; Kang, D.-M.; Kim, Y.-H.; Park, C. E.; Kwon, S.-K. *Macromolecules* **2010**, *43*, 2118. (e) Wagner, K.; Crowe, L. L.; Wagner, P.; Gambhir, S.; Partridge, A. C.; Earles, J. C.; Clarke, T. M.; Gordon, K. C.; Officer, D. L. *Macromolecules* **2010**, *43*, 3817. (f) Yu, C.-Y.; Ko, B.-T.; Ting, C.; Chen, C.-P. *Sol. Energy Mater. Sol. Cells* **2009**, *93*, 613.

(11) Zhang, Z.-G.; Zhang, S. Y.; Min, J.; Chui, C. H.; Zhang, J.; Li, Y. F. *Macromolecules* **2012**, *45*, 113−118.

(12) Sun, H. *J. Phys. Chem. B* **1998**, *102*, 7338.

(13) (a) Zhang, Z.-G.; Zhang, K.-L.; Liu, G.; Zhu, C.-X.; Neoh, K.-G.; Kang, E.-T. *Macromolecules* **2009**, *42*, 3104. (b) Zhang, Z.-G.; Liu, Y.-

L.; Yang, Y.; Hou, K.; Peng, B.; Zhao, G. J.; Zhang, M. J.; Guo, X.; Kang, E.-T.; Li, Y. F. *Macromolecules* **2010**, *43*, 9376. (c) Zhang, Z.-G.; Fan, H. J.; Min, J.; Zhang, S.; Zhang, J.; Zhang, M. J.; Guo, X.; Zhan, X. W.; Li, Y. F. *Polym. Chem.* **2011**, *2*, 1678. (d) Zhang, Z.-G.; Yang, Y.; Zhang, S. Y.; Min, J.; Zhang, J.; Zhang, M. J.; Guo, X.; Li, Y. F. *Synth. Met.* **2011**, *161*, 1383.

(14) (a) Huang, F.; Chen, K.-S.; Yip, H.-L.; Hau, S. K.; Acton, O.; Zhang, Y.; Luo, J.; Jen, A. K. Y. *J. Am. Chem. Soc.* **2009**, *131*, 13886−13887. (b) Duan, C.; Cai, W.; Huang, F.; Zhang, J.; Wang, M.; Yang, T.; Zhong, C.; Gong, X.; Cao, Y. *Macromolecules* **2010**, *43*, 5262−5262. (c) Hsu, S.-L.; Chen, C.-M.; Wei, K.-H. *J. Polym. Sci., Part A: Polym. Chem.* **2010**, *48*, 5126−5134. (d) Cheng, Y.-J.; Hung, L.-C.; Cao, F.-Y.; Kao, W.-S.; Chang, C.-Y.; Hsu, C.-S. *J. Polym. Sci., Part A: Polym. Chem.* **2011**, *49*, 1791−1801. (e) Sahu, D.; Padhy, H.; Patra, D.; Huang, J.-H.; Chu, C.-W.; Lin, H.-C. *J. Polym. Sci., Part A: Polym. Chem.* **2010**, *48*, 5812−5823.

(15) Wadsworth, W. S.; Emmons, W. D. *J. Am. Chem. Soc.* **1961**, *83*, 1733.

(16) Carsten, B.; He, F.; Son, H. J.; Xu, T.; Yu, L. *Chem. Rev.* **2011**, *111*, 1493.

(17) Sun, Q. J.; Wang, H. Q.; Yang, C. H.; Li, Y. F. *J. Mater. Chem.* **2003**, *13*, 800.

(18) Gaussian 03, R. E.; Frisch, M. J.; Trucks, G. W.; Schlegel, H. B.; Scuseria, G. E.; Robb, M. A.; Cheeseman, J. R.; Montgomery, J. A.; Vreven, J., T.; Kudin, K. N.; Burant, J. C.; Millam, J. M.; Iyengar, S. S.; Tomasi, J.; Barone, V.; Mennucci, B.; Cossi, M.; Scalmani, G.; Rega, N.; Petersson, G. A.; Nakatsuji, H.; Hada, M.; Ehara, M.; Toyota, K.; Fukuda, R.; Hasegawa, J.; Ishida, M.; Nakajima, T.; Honda, Y.; Kitao, O.; Nakai, H.; Klene, M.; Li, X.; Knox, J. E.; Hratchian, H. P.; Cross, J. B.; Bakken, V.; Adamo, C.; Jaramillo, J.; Gomperts, R.; Stratmann, R. E.; Yazyev, O.; Austin, A. J.; Cammi, R.; Pomelli, C.; Ochterski, J. W.; Ayala, P. Y.; Morokuma, K.; Voth, G. A.; Salvador, P.; Dannenberg, J. J.; G., Z. V.; Dapprich, S.; Daniels, A. D.; Strain, M. C.; Farkas, O.; Malick, D. K.; Rabuck, A. D.; Raghavachari, K.; Foresman, J. B.; Ortiz, J. V.; Cui, Q.; Baboul, A. G.; Clifford, S.; Cioslowski, J.; Stefanov, B. B.; Liu, G.; Liashenko, A.; Piskorz, P.; Komaromi, I.; Martin, R. L.; Fox, D. J.; Keith, T.; Al-Laham, M. A.; Peng, C. Y.; Nanayakkara, A.; Challacombe, M.; Gill, P. M. W.; Johnson, B.; Chen, W.; Wong, M. W.; Gonzalez, C.; Pople, J. A. Gaussian, Inc.: Wallingford CT, 2004.

(19) Asawapirom, U.; Güntner, R.; Forster, M.; Farrell, T.; Scherf, U. *Synthesis 2002* **2002**, 1136.